Monthly Notices of the ROYAL ASTRONOMICAL SOCIETY
MNRAS **444,** 3802–3808 (2014) doi:10.1093/mnras/stu1687

Simultaneous optical and near-IR photometry of 4U1957+115 - a missing secondary star

Pasi Hakala,[1]★ Panu Muhli[2] and Phil Charles[3,4]

[1]*Finnish Centre for Astronomy with ESO (FINCA), University of Turku, Väisäläntie 20, FI-21500 Piikkiö, Finland*
[2]*National Land Survey of Finland, PL 84, FI-00521 Helsinki, Finland*
[3]*School of Physics and Astronomy, University of Southampton, Highfield, Southampton SO17 1BJ, UK*
[4]*Astrophysics, Cosmology and Gravity Centre (ACGC), University of Cape Town, Private Bag X3, Rondebosch 7701, South Africa*

Accepted 2014 August 15. Received 2014 July 28; in original form 2014 February 21

ABSTRACT

We report the results of quasi-simultaneous optical and near-IR (NIR) photometry of the low-mass X-ray binary, 4U 1957+115. Our observations cover the *B, V, R, I, J, H* and *K*-bands and additional time series NIR photometry. We measure a spectral energy distribution (SED), which can be modelled using a standard multitemperature accretion disc, where the disc temperature and radius follow a power-law relation. Standard accretion disc theory predicts the power-law exponent to be −3/4, and this yields, perhaps surprisingly, acceptable fits to our SED. Given that the source is a persistent X-ray source, it is however likely that the accretion disc temperature distribution is produced by X-ray heating, regardless of its radial dependence. Furthermore, we find no evidence for any emission from the secondary star at any wavelength. However, adding a secondary component to our model allows us to derive a 99 per cent lower limit of 14 or 15 kpc based on Monte Carlo simulations and using either an evolved K2 or G2V secondary star, respectively. In >60 per cent of cases, the distance is >80 kpc. Such large distances favour models with a massive (>15 $M_\odot$) black hole primary. Our quasi-simultaneous *J*- and *V*- band time series photometry, together with the SED, reveals that the optical/NIR emission must originate in the same region, i.e. the accretion disc. The likely extreme mass ratio supports suggestions that the accretion disc must be precessing which, depending on the length of the precession period, could play a major part in explaining the variety of optical light-curve shapes obtained over the last two decades.

Key words: accretion, accretion discs – stars: black holes – stars: distances – X-rays: binaries.

1 INTRODUCTION

4U 1957+115 (V1408 Aql) is a persistently bright low-mass X-ray binary (LMXB). It was first detected by *Uhuru* (Giacconi et al. 1974), and its optical counterpart was later identified by Margon, Thorstensen & Bowyer (1978). The source also appears in an early list of black hole candidates (BHC; White & Mason 1985), as it shows an ultrasoft X-ray spectrum (White & Marshall 1984), but currently there is no firm evidence on the nature of the compact object. The source was noted to vary in the optical (Motch et al. 1985), and Thorstensen (1987) discovered a 9.33 h sinusoidal *V*-band modulation. This period, if of orbital origin, implies that a Roche lobe filling, main-sequence donor would have a mass of $\sim 0.11 \times P_{\rm orb}(h) = 1.0\ M_\odot$. Intriguingly, no optical spectroscopic signature of the donor has been found (Shahbaz et al. 1996).

Observations by a variety of X-ray missions have painted a mixed picture for the nature of the compact object. Earlier studies (Yaqoob, Ebisawa & Mitsuda 1993; Singh, Apparao & Kraft 1994) favour a neutron star (NS) model, whilst more recent work seems to suggest a black hole (BH) primary (Ricci, Israel & Stella 1995; Wijnands, Miller & van der Klis 2002; Nowak et al. 2008, 2012). Nowak & Wilms (1999) compare the merits of both models and suggest that the source probably contains a warped precessing disc, as also suggested by Hakala, Muhli & Dubus (1999, hereafter HMD99) based on long-term changes in the optical orbital light curve. Recent optical studies have produced mixed results, with Russell et al. (2010) reporting a non-detection for the optical period, and Bayless et al. (2011) claiming a pure sinusoidal modulation due to the X-ray heating of the secondary.

There is no clear X-ray modulation over the orbital period. However, the X-ray luminosity varies by a factor of ∼3 over a time-scale of a few months (Nowak & Wilms 1999). Furthermore, there is some tentative evidence for a 117 d or 250–260 d superorbital period from *RXTE* All Sky Monitor (*RXTE* ASM) data (Nowak & Wilms 1999). Recent *Chandra*, *XMM–Newton*, *RXTE* and *Suzaku* observations by Nowak et al. (2008, 2012) suggest that the system contains a rapidly rotating BH, the mass of which hinges on determining the distance to the system.

★ E-mail: pahakala@utu.fi

Table 1. 4U 1957+115 *J*-band time series observing log.

Start date	Exposure (s)	Length (d)	Phase	Filter
2452477.4755	210×(10×6)	0.20	0.00–0.51	*J*
2452478.4397	260×(10×6)	0.25	0.48–1.12	*J*
2452479.4712	180×(10×6)	0.23	0.13–0.72	*J*

Phase has an arbitrary zero-point on the 9.33 h period. Observations from the first two nights were used to construct the SED. Additionally, four *V*-band points were obtained during the *J*-band time series observations.

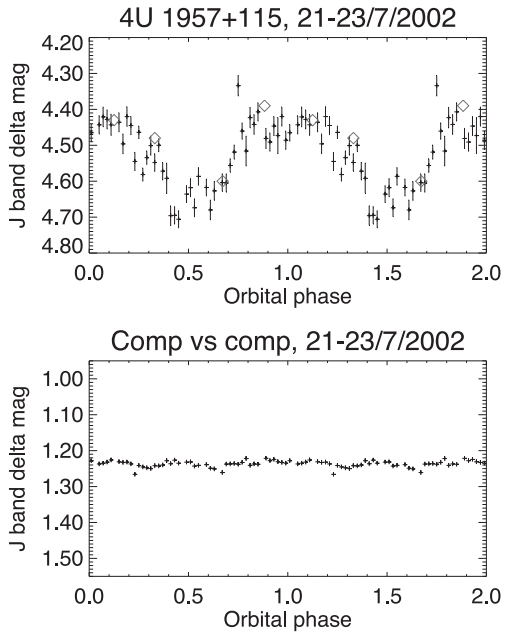

Figure 1. The 2002 July 21–23 *J*-band data folded on the 9.33 h orbital period (top). The grey diamonds denote quasi-simultaneous *V*-band observations shifted to the same delta magnitude range. The lower plot shows the delta magnitude between two comparison stars in the same field.

2 OBSERVATIONS

We have observed the source with the 2.5 m Nordic Optical Telescope (NOT) located at the Roque de los Muchachos observatory, La Palma, using a combination of StanCam and NOTCam on 2002 July 21–23 (details in Table 1). StanCam is a stand-by optical CCD located within the Cassegrain instrument rotator of NOT and consists of a TEK 1024 × 1024 back-side illuminated thinned CCD with a 3 arcmin × 3 arcmin field of view. It is always available and is fed though a 45 deg insertable flat mirror. NOTCam is a near-IR (NIR) camera operated at the Cassegrain focus. It is based on a 1024 × 1024 Rockwell 'Hawaii' HgCdTe array and has a field of view of 4 arcmin × 4 arcmin.

These two instruments can be operated in a quasi-simultaneous mode taking exposures in both optical and NIR bands in a sequence. We have obtained exposures in the *B, V, R, I, J, H* and *K* bands together with a time series in the *J* and *V* bands (Fig. 1). Both the optical and NIR observations have been reduced using IRAF and standard reduction techniques. A multipoint dithering mode was used in the NIR. Further details of the time series observations can be found in Table 1. In order to calibrate the optical and NIR observations, several standard stars were observed. In particular, we used five NIR standards from Hunt et al. (1998) to calibrate the *J*, *H* and *K* magnitudes. The spectral energy distribution (SED), tabulated in Table 2 and plotted in Fig. 2, is based on aperture photometry using the standard 'PHOT' task of IRAF.

Table 2. The SED of 4U 1957+115.

Filter	Flux (erg Å^{-1} cm^{-2} s^{-1})	Magnitude
B	$16.6 \pm 0.78 \times 10^{-17}$	18.97 ± 0.05
V	$9.67 \pm 0.27 \times 10^{-17}$	18.95 ± 0.03
R	$6.35 \pm 0.30 \times 10^{-17}$	18.70 ± 0.05
I	$3.24 \pm 0.15 \times 10^{-17}$	18.66 ± 0.05
J	$1.47 \pm 0.10 \times 10^{-17}$	18.32 ± 0.07
H	$0.64 \pm 0.061 \times 10^{-17}$	18.15 ± 0.10
K	$0.22 \pm 0.026 \times 10^{-17}$	18.15 ± 0.12

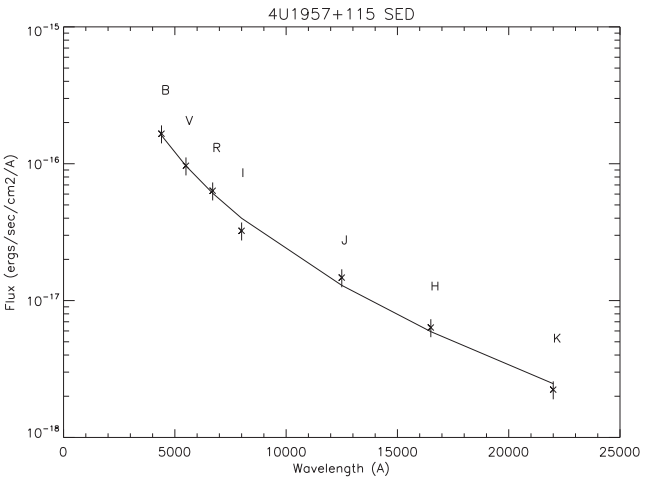

Figure 2. The *B*, *V*, *R*, *I*, *J*, *H*, *K* SED of 4U 1957+115, together with our accretion disc model. See the text for details.

3 MODELLING THE SED

The resulting SED, plotted in Fig. 2, shows a very blue continuum. This is in accordance with the low hydrogen column density of 1.0–1.1 × 10^{21} estimated from the X-ray spectra (Nowak et al. 2008) and thus the interstellar extinction is small (it is still included in our modelling as a free parameter).

Simple visual examination of the shape of the SED appears to suggest that there might be a slightly different power-law slope for the optical (*B*, *V*, *R*, *I*) and the NIR (*J*, *H*, *K*) bands. This would be expected from a cool, low-mass donor. However, we will show in subsequent modelling that this clearly is not the case.

In order to quantify the level of any contribution by the secondary star, and to investigate the origin of the continuum, we have proceeded to fit it initially with a traditional accretion disc model (Shakura & Sunyaev 1973), where we assume an optically thick disc with a radial power-law temperature dependence. The model consists of annular rings whose temperature varies only as a power law with radius from the centre. In order to keep our model simple enough, we have fixed the ratio of inner and outer disc radii to 0.01. We are thus excluding the inner 0.01 per cent of the disc area. Selecting a different ratio (e.g. 0.001) did not affect the results significantly, since the contribution from the excluded area is very small. We still retain the same disc temperature profile, i.e. the T_e at 0.01 radius remains the same.

The free parameters are the disc inner radius temperature and the power-law index α that determines the dependence of local disc temperature on the disc radius, i.e. $T_e(r) \propto r^{\alpha}$ and the amount of interstellar extinction $E(B-V)$.

We are unable to obtain a formally good fit to the data using the errors given in Table 2. The values of these typically range from 3–5 per cent in optical to 11 per cent in the K band. The scatter of our data about the best fit suggests that the formal error is not sufficient and does not contain all the systematics, which are likely to be dominated by the intrinsic flickering/variability of the accreting source, as demonstrated in both previous and current (e.g. Fig. 1) light curves. Note that the different photometric bands were obtained in a sequence, not simultaneously. We have taken this into account by examining the residuals to the fit and have increased the errors in each band to 15 per cent. After doing this, we find that we can fit the SED with an accretion disc model, as described above, and a best fit is overplotted in Fig. 2.

We have determined the errors for the fit parameters and further examined the correlations and the parameter space in general by carrying out a Monte Carlo analysis. This involved creating 20 000 synthetic data sets (SEDs) based on a best fit (and the 15 per cent errors) and fitting these with the model. This exercise revealed that different combinations of fitting parameters are capable of producing equally good fits, since the inner disc temperature and the radial temperature index α are correlated. This led to a bimodal distribution of possible models, where we could typically fit the SED either using a low inner disc temperature of the order of 10 000–15 000 K coupled with a very steep temperature profile and rather unphysical normalizations or an inner disc temperature of 70 000–90 000 K with $\alpha = -0.75$. The first option is not physical, since it would imply impossibly low disc temperatures for most of the disc. Single blackbody temperature fits are also ruled out and the effect of interstellar reddening is found to be negligible.

Secondly, we have experimented by adding a solar-like 5800 K (blackbody) component to the model to see whether including/forcing a secondary in the fit would change the temperature distribution of the resulting accretion disc model and in order to derive upper limits for the emission from the secondary. In this case, we could fit the SED also with a uniform temperature disc, but the model for any contribution from the secondary is not physical, since it requires the secondary star projected area to be an order of magnitude larger than that of the whole accretion disc.

In conclusion, we can model the SED using an inner disc temperature of 81 000 ± 26 000 K together with a conventional radial temperature dependence value for the power law, i.e. $\alpha = -0.75$ and $E(B-V) = 0.0 \pm 0.07$, $\chi^2 = 3.92$, 2 degrees of freedom (d.o.f.; $p = 0.14$). No contribution from the secondary star is required for this fit.

3.1 The secondary star

Given the reasonable fits to the SED by the accretion disc emission model alone, it is evident that the emission from the secondary star must be marginal and there is no clear visual detection of the secondary in our data. In order to obtain upper limits for the emission from the secondary (and thus lower limit for the source distance), we have employed two approaches. First, we have used our basic accretion disc model fits (as described above, no secondary included) and measured the scatter (standard deviation) in our K-band model flux from the model fits to our synthetic, i.e. Monte Carlo, data sets. We then use this scatter to derive a 3σ upper limit for the K-band flux from the secondary. The resulting value is 9.0×10^{-19} erg cm^{-2} s^{-1} Å^{-1}, which corresponds to a minimum distance of 15 kpc (assuming a solar-type secondary) or 13 kpc (assuming an evolved 5000 K secondary).

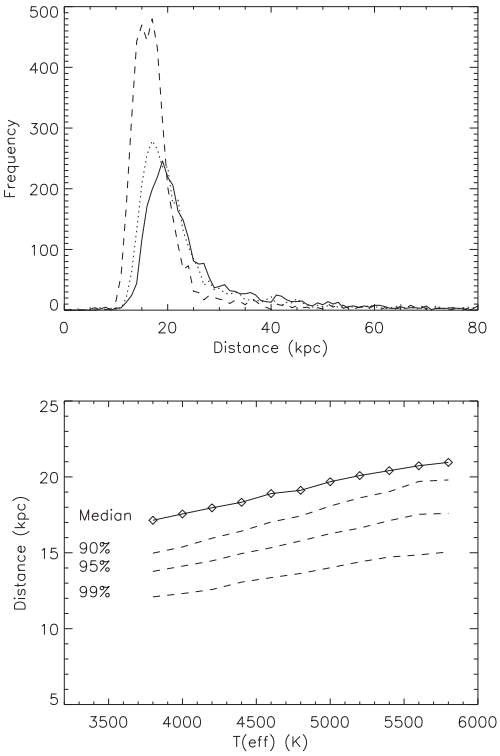

Figure 3. Top: the probability distributions of the distance to 4U 1957+115 based on the 10 000 Monte Carlo simulated synthetic SEDs fitted with models including a 5800 K blackbody component representing a solar-type secondary star (solid line), a slightly evolved secondary (K2, 5000 K – dotted line) and a heavily evolved secondary (3800 K – dashed line). Note that in >60 per cent of cases (no detection of the secondary) the distance is >80 kpc. Bottom: the median distance (in the case when a secondary is detected) and the 90, 95 and 99 per cent lower limits for the distance to 4U 1957+115 as a function of secondary spectral type based on 11 × 10 000 Monte Carlo simulations. Note that the median distance refers to the median of cases where the secondary has a significant contribution (i.e. distance <50 kpc).

As a second method, we have added an extra 5800 K blackbody component to our model and fitted the SED with this more complex model and then carried out Monte Carlo simulations based on the fit in order to derive a probability distribution for the flux originating from the secondary. This was then transformed into a probability distribution of distance by adopting a solar absolute K magnitude of 3.33 (Worthey 1994). The resulting probability distribution peaks at 19 kpc (Fig. 3, top). We can also measure the 1 per cent lower percentile at 15 kpc. Naturally, we cannot give any upper limit for the distance, given that there is no firm detection of the secondary in the SED. Actually, in about >60 per cent of cases in our Monte Carlo simulations, there is no significant flux from the secondary. The source distance probability distribution tail corresponding to these >60 per cent is off-scale (i.e. >80 kpc) in Fig. 3.

The results from our two different approaches to estimate the minimum distance of 4U 1957+115 seem to agree with each other (∼15 kpc). Naturally, these depend on the assumption that the secondary is of solar spectral and luminosity class. However, we know from the studies of secondary stars in cataclysmic variables

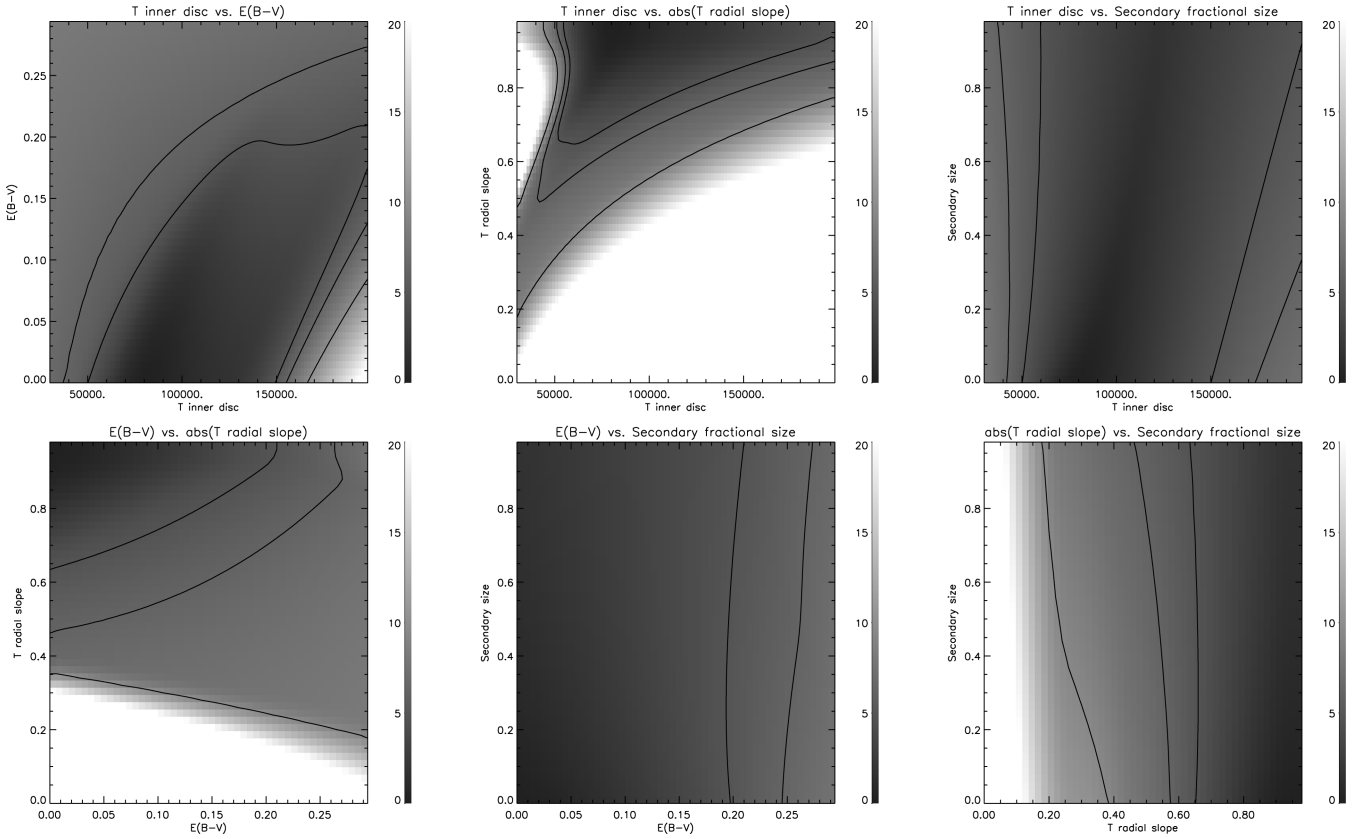

Figure 4. The $\Delta\chi^2$ distribution maps and confidence contours for various parameter pairs. The darkest areas correspond to the minimum χ^2 regions. We also show 90, 95 and 99 per cent confidence contours obtainable from our SED fits. The results are obtained from a 100×50×50×50 grid of models covering the parameter ranges indicated in the plots.

of similar orbital periods that the Roche lobe filling secondaries are typically somewhat evolved (Beuermann et al. 1998; Knigge 2006). We estimate, using the empirical spectral-type versus orbital period distribution of Knigge (2006), that the characteristic spectral type for the secondary is K2, i.e. the effective temperature would be around 5000 K. Lowering the blackbody temperature to 5000 K would have an approximate effect of a 30 per cent drop in the *K*-band flux (retaining the same radius for the secondary and approximating it as a blackbody). This would decrease the minimum distance from 15 kpc by about 15 per cent to 13 kpc. To further demonstrate this, we have carried out the previously described Monte Carlo analysis using a range of (fixed) secondary effective temperatures from 3800 K (M0) to 5800 K (G2). The resulting distance distributions for 3800, 5000 and 5800 K cases are shown in the top panel of Fig. 3, whilst the median distance (of the cases where the secondary is detected), together with the 90, 95 and 99 per cent lower limits as a function of secondary effective temperature, is shown in the bottom plot of Fig. 3. Finally, given these lower limits to the distance, it is worth noting that in most cases of our Monte Carlo simulations the secondary is not detected and that the 1 per cent lower percentile limits for the distance are 15 and 14 kpc for the solar-type and K2 secondaries, respectively. The resulting distance probability distribution (Fig. 3, top) is also highly skewed, setting very strict lower limits for the distance.

We have also carried out a confidence region analysis in $\Delta\chi^2$ space in order to visualize the limits and correlations between the fit parameters. The results of this exercise are shown in Fig. 4 and discussed further in Section 5.

3.2 The effects of disc irradiation and extinction

In order to further examine the validity of our modelling described above, we have also carried out SED modelling using an approach introduced by Hynes et al. (2002). Their model consists basically of two power-law distributions for the disc radial temperature, i.e. one for the viscous disc ($\alpha = -3/4$) and another for the irradiated disc ($\alpha = -3/7$; see Hynes et al. 2002 for details). The free parameters are the outer disc temperatures for the 'viscous power law' and the 'irradiated power law' together with a normalization term. The main difference to our modelling is that the power-law indices are fixed. As a result, we find that the 'irradiated power-law' component will be attenuated in the fitting process and we are left with only the viscous (i.e. $\alpha = -3/4$) power law, thus producing the same best-fitting model as in our original modelling. Exactly the same happens if we add a secondary component to the Hynes et al. (2002) model. In practice, the outer disc temperature of the 'irradiated power law' ($\alpha = -3/7$) will be forced towards zero by the fitting process.

Extinction is a free parameter in our fits and both our model and the Hynes et al. model favour $E(B-V) = 0.0$. This is somewhat surprising, given that both the X-ray spectral fits (Nowak et al. 2008) and the NASA/IPAC extinction estimates [based on Schlegel, Finkbeiner & Davis (1998) dust maps] indicate $E(B-V) = 0.2$ and 0.175, respectively. However, our confidence region analysis (Fig. 4) shows that even if $E(B-V) = 0.0$ yields the best fits, $E(B-V) = 0.2$ solutions still lie within the 90 per cent confidence region for our models. We have also tried forcing $E(B-V) = 0.175$ in our fits, but this makes the fits considerably worse

(χ^2 becomes 7.86 instead of 3.92, 2 d.o.f.). If we allow for much steeper radial temperature distributions, we can achieve equally good fits with $E(B-V) = 0.175$, but this requires a disc inner edge temperature of 3.6×10^5 K combined with a very steep radial temperature distribution of $\alpha = -1.5$. In this case, we obtain $\chi^2 = 3.97$ (2 d.o.f.). However, there are no clear physical grounds for such an extreme α value.

4 TIME SERIES PHOTOMETRY

In addition to obtaining the multicolour optical NIR magnitudes, we have also monitored the system in *J*, with interleaved *V* measurements at regular intervals (see Table 1). The motivation for this was to study whether the same 9.33 h modulation that appeared to have no colour dependence in *UBVRI* (HMD99) would continue in the NIR.

We have folded our *J*-band photometry, together with the quasi-simultaneous *V*-band data, over the 9.33 h cycle (presumed to be the orbital period) in Fig. 1. The *J*-band full amplitude is ∼0.25 mag, similar to that observed by Thorstensen (1987) in the optical, but much lower than observed by HMD99. However, the light-curve shape, with different gradients for the decline and rise phases, is more similar to that detected by HMD99 than the sinusoidal light curve seen by Thorstensen (1987) or Bayless et al. (2011). It is clear that the light-curve profile shows long-term evolution, possibly related to a precessional cycle of the accretion disc. Our *V*-band data points seem to follow the *J*-band modulation. This agrees with HMD99, where all the colours (*UBVRI*) seemed to show very similar modulation over the orbital period.

5 DISCUSSION

Several papers (Thorstensen 1987; HMD99; Russell et al. 2010; Bayless et al. 2011; Mason et al. 2012) have reported results of optical studies of the system with rather varied conclusions about the origin of the optical variability. In summary, it appears that the amplitude of orbital variability can range from zero to 0.6 mag full amplitude. In order to accommodate such large changes, the origin of the emission must be flexible in nature. Since 4U 1957+115 is a persistent X-ray source, such changes cannot be produced by a model where the sole driving mechanism for the optical variability is the X-ray heating of the secondary star, as suggested by Bayless et al. (2011). This point is further underlined by our optical–NIR SED, the modelling of which requires a very significant temperature gradient in the disc. Such a temperature gradient cannot be achieved on the surface of an X-ray heated secondary star. In addition, the almost identical variability amplitude seen in all the light curves, from UV to NIR (HMD99), and our quasi-simultaneous *V*- and *J*-band light curves presented in this study, also points to the accretion disc as a source of most of the optical and NIR emission.

The *RXTE* ASM light curve of 4U 1957+115 has shown evidence for ∼117d superorbital period (Nowak & Wilms 1999). It is thus feasible that the different optical light-curve shapes observed by different authors are a consequence of observing the system at different superorbital phases. If the source indeed harbours a BH, the accretion disc would be susceptible to tidal instabilities due to the extreme mass ratio, and precession of the disc would follow (Whitehurst & King 1991). Similar changes in accretion disc structure, as evidenced by changing optical light-curve shapes, are fairly common in LMXBs and have been observed in several systems such as Her X-1 (Gerend & Boynton 1976), UW CrB (Hakala et al. 1998, 2009), 4U 1916−05 (Callanan 1993; Homer et al. 2001), AC 211 (Auriere et al. 1989; Ilovaisky 1989), EXO 0748−676 (Pearson et al. 2006) and GR Mus (Cornelisse et al. 2013) to name just a few.

It is rather peculiar that the SED modelling seems to require a rather steep temperature distribution with $\alpha = -0.75$. Even if such a distribution is predicted for purely viscous heating of an accretion disc (Shakura & Sunyaev 1973), a much flatter distribution (i.e. $\alpha = -0.5$) would be expected for a persistent X-ray source irradiating the disc (King 1998). However, if the irradiating X-ray source lies above the orbital (and disc) plane and the disc is mostly confined to the orbital plane, an extra $1/r$ term is required to account for the disc projected area as seen by the X-ray source. Thus, the X-ray heating per disc unit surface area would follow $F_{\rm X} \propto 1/r^3$, and assuming local thermodynamic equilibrium ($F_{\rm X} \propto T_{\rm e}^4$), the disc surface temperature $T_{\rm e}$ would follow $T_{\rm e} \propto r^{-3/4}$ (Hynes 2014). This means that for a realistic disc (i.e. a disc that is partly warped out of the orbital plane and heated by an X-ray source above the disc) we expect the X-ray heating to follow $F_{\rm X} \propto 1/r^n$, where $n = 2$–3 (i.e. $T_{\rm e} \propto r^{\alpha}$, where $\alpha = [-0.75, -0.5]$). We limited α to be > -0.75 in our fits to keep the results within physical bounds, but still found that the SED fits were typically pegged to this hard lower limit. It is however possible that a convex inner disc structure or warping in the inner disc could shield the outer disc from irradiation, resulting in a much steeper temperature gradient than theoretically expected (Dubus et al. 1999). Similarly, if only the inner disc is surrounded by an X-ray scattering hot accretion disc corona (ADC), the scattered X-rays, depending on the ADC optical depth and size, will preferentially heat the part of the disc within the ADC radius. In fact, our grid-based exploration of the parameter space (Fig. 4) covered an α range of $[-1.0, 0.0]$ and showed that the best fits could be obtained with the steepest temperature distributions, thereby pointing towards extra heating in the inner disc. Finally, we would like to point out that, apart from the grid-based computations (Fig. 4) where a wide parameter space was systematically explored, the maximum area of the secondary star in the fits was limited to 1/3 of the projected area of the accretion disc. This is a reasonable assumption since, for instance, taking a likely value of $q = 0.1$ (assuming a BH system) the Roche lobe area of the secondary becomes about 10–15 per cent of the accretion disc area. Now, assuming a flat disc and maximum inclination of 70° (no eclipses are observed) will bring this fraction up to 30–35 per cent. Without such limitation, the best-fitting model would include a secondary 10–50 times the size of the accretion disc together with a very steep hot disc continuum, which is clearly not physical.

It is interesting to note that taking our accretion disc model of the SED and extrapolating the temperature distribution inwards yields a maximum disc temperature of 0.8–0.9 keV at the Schwarzschild radius for a 15 $M_\odot$ BH. This is in agreement with the maximum disc temperatures seen in BH binaries. Nowak et al. (2008) list disc blackbody (XSPEC model *diskbb*) temperatures in the range 1.2–1.8 keV for 4U 1957+115. Given the uncertainties involved in our extrapolation, these values are in agreement with our model. It is thus feasible that all the emission ranging from soft X-rays to NIR can be explained largely by a single multitemperature accretion disc model with the standard radial disc temperature profile proportional to $r^{-3/4}$. Similar results have been obtained by Russell et al. (2011), who find that the broad-band (radio to X-ray) SED can be modelled with thermal emission from a multitemperature accretion disc alone. The common IR excess, attributed to synchrotron emission seen in many BH X-ray binaries (XRBs) in outburst (Russell et al. 2006), is not detected. The likely reason is that the source is in a persistent soft state, with no radio jet emission (Russell et al. 2011). This is in agreement with our preferred model, where the optical/NIR

modulation is due to the changing projected area of either a warped or flared accretion disc over the orbital period and there is no significant contribution to the optical/NIR emission from the secondary star.

Our 99 per cent lower limit for the distance of the source is ∼15 kpc. This, together with the Galactic latitude of 9.3 deg, places the system 2.5 kpc above the Galactic plane and at about 12 kpc from the Galactic centre, making it a distant Galactic halo object. Adopting a distance of 18 kpc (peak in the probability distribution, Fig. 3) and taking the 0.7–8 keV X-ray flux of 1.0 10^{-9} erg cm^{-2} s^{-1} from Nowak et al. (2012) would then imply an X-ray luminosity $L_X = 3.8\ 10^{37}$ erg s^{-1} which is about 15 per cent of the Eddington limit for a 1.4 $M_\odot$ NS (or less than 2.5 per cent for a 16 $M_\odot$ BH). Russell et al. (2010) examine the X-ray–optical luminosity ratio of 4U 1957+115 in comparison with a variety of XRBs. They conclude that if the distance is more than 20 kpc, the source is likely to contain a BH (or possibly an NS atoll source if the distance is of the order of 20 kpc). Our data are thus inconclusive regarding the nature of the compact object, even if in about 80 per cent of cases in our Monte Carlo study the distance is above ∼20 kpc.

There now appears to be a small population of short-period (2–5 h) BHC known in the Galactic halo (Shaw et al. 2013), all of which are X-ray transients and most of which are substantially sub-Eddington for their (dynamically) determined masses. If the high mass of the compact object in 4U 1957+115 can be confirmed, the source would be the first persistent, and the longest period, BHC to join this population. It is worth noting that based on its X-ray luminosity (and inferred accretion rate), 4U 1957+115 is likely to be a persistent source according to the disc instability models (Coriat, Fender & Dubus 2012).

6 CONCLUSIONS

We have modelled the *BVRIJHK*-SED of 4U 1957+115 with an accretion disc model that allows for different radial temperature profiles, i.e. different disc heating mechanisms. Our results are in agreement with a viscously heated disc, but given the uncertainties involved in the expected irradiatively heated disc profile and the persistency of the X-ray source, we still believe that the X-ray heating of the disc must play a major role.

Furthermore, modelling our optical and NIR photometry with a multitemperature accretion disc model together with a solar-type secondary yields a 99 per cent minimum distance of 15 (14) kpc to 4U 1957+115. The value in parentheses corresponds to an evolved K2 secondary. This distance is broadly in agreement with the 16 $M_\odot$ BH models with spin parameter $a^* \sim 1$ and spectral hardening factor of $h_d = 1.4$ as proposed by Nowak et al. (2008). Our quasi-simultaneous *J*- and *V*-band photometry confirms that the optical and NIR emission indeed come from a common location, i.e. the accretion disc. This means that the time-dependent/long-term changes in the optical and NIR orbital modulation are likely caused by changing orientation of the precessing accretion disc within the binary rest frame. Simultaneous optical and NIR observations, as well as a high-resolution NIR spectroscopic search for a signature of the donor, would be highly desirable in order to build up a more coherent picture of the underlying spectral model and put even more stringent limits on the secondary star and the distance to 4U 1957+115. This is particularly important since our current set of data is only broadly consistent with the independent extinction estimates towards the object and we particularly need more simultaneous UV and optical data.

ACKNOWLEDGEMENTS

This work is based on observations made with the Nordic Optical Telescope, operated by the Nordic Optical Telescope Scientific Association at the Observatorio del Roque de los Muchachos, La Palma, Spain, of the Instituto de Astrofisica de Canarias. This research has made use of the NASA/IPAC Infrared Science Archive, which is operated by the Jet Propulsion Laboratory, California Institute of Technology, under contract with the National Aeronautics and Space Administration. We would like to thank the anonymous referee for input that made the final paper significantly better.

REFERENCES

Auriere M., Ilovaisky S. A., Koch-Miramond L., Chevalier C., Cordoni J.-P., 1989, in Battrick B., Hunt J., eds, ESA SP-1: The 23rd ESLAB Symposium on Two Topics in X Ray Astronomy. ESA, Noordwijk, p. 267
Bayless A. J., Robinson E. L., Mason P. A., Robertson P., 2011, ApJ, 730, 43
Beuermann K., Baraffe I., Kolb U., Weichhold M., 1998, A&A, 339, 518
Callanan P. J., 1993, PASP, 105, 961
Coriat M., Fender R. P., Dubus G., 2012, MNRAS, 424, 1991
Cornelisse R., Kotze M. M., Casares J., Charles P. A., Hakala P. J., 2013, MNRAS, 436, 910
Dubus G., Lasota J.-P., Hameury J.-M., Charles P. A., 1999, MNRAS, 303, 139
Gerend D., Boynton P. E., 1976, ApJ, 209, 562
Giacconi R., Murray S., Gursky H., Kellogg E., Schreier E., Matilsky T., Koch D., Tananbaum H., 1974, ApJS, 27, 37
Hakala P. J., Chaytor D., Vilhu O., Piirola V., Morris S. L., Muhli P., 1998, A&A, 333, 540
Hakala P. J., Muhli P., Dubus G., 1999, MNRAS, 306, 701 (HMD99)
Hakala P. J., Hjalmarsdotter L., Hannikainen D. C., Muhli P., 2009, MNRAS, 394, 892
Homer L., Charles P. A., Hakala P., Muhli P., Shih I.-C., Smale A. P., Ramsay G., 2001, MNRAS, 322, 827
Hunt L. K., Mannucci F., Testi L., Migliorini S., Stanga R. M., Baffa C., Lisi F., Vanzi L., 1998, AJ, 115, 2594
Hynes R. I., 2014, in Gonzalez Martinez-Pais G., Shahbaz T., Casares Velazquez J., eds, Accretion Processes in Astrophysics, XXI Canary Islands Winter School of Astrophysics. Cambridge Univ. Press, New York, preprint (astro-ph/1010.5770)
Hynes R. I., Haswell C. A., Chaty S., Shrader C. R., Cui W., 2002, MNRAS, 331, 169
Ilovaisky S., 1989, in Battrick B., Hunt J., eds, ESA SP-1: The 23rd ESLAB Symposium on Two Topics in X Ray Astronomy. ESA, Noordwijk, p. 145
King A. R., 1998, MNRAS, 296, L45
Knigge C., 2006, MNRAS, 373, 484
Margon B., Thorstensen J. R., Bowyer S., 1978, ApJ, 221, 907
Mason P. A., Robinson E. L., Bayless A. J., Hakala P. J., 2012, AJ, 144, 108
Motch C., Chevalier C., Ilovaisky S. A., Pakull M. W., 1985, Space Sci. Rev., 40, 239
Nowak M. A., Wilms J., 1999, ApJ, 522, 476
Nowak M. A., Juett A., Homan J., Yao Y., Wilms J., Schulz N. S., Canizares C. R., 2008, ApJ, 689, 1199
Nowak M. A., Wilms J., Pottschmidt K., Schulz N., Maitra D., Miller J., 2012, ApJ, 744, 107
Pearson K. J. et al., 2006, ApJ, 648, 1169
Ricci D., Israel G. L., Stella L., 1995, A&A, 299, 731
Russell D. M., Fender R. P., Hynes R. I., Brocksopp C., Homan J., Jonker P. G., Buxton M. M., 2006, MNRAS, 371, 1334
Russell D. M., Lewis F., Roche P., Clark J. S., Breedt E., Fender R. P., 2010, MNRAS, 402, 2671

Russell D. M., Miller-Jones J. C. A., Maccarone T. J., Yang Y. J., Fender R. P., Lewis F., 2011, ApJ, 739, L19
Schlegel D. J., Finkbeiner D. P., Davis M., 1998, ApJ, 500, 525
Shahbaz T., Smale A. P., Naylor T., Charles P. A., van Paradijs J., Hassall B. J. M., Callanan P., 1996, MNRAS, 282, 1437
Shakura N. I., Sunyaev R. A., 1973, A&A, 24, 337
Shaw A. W. et al., 2013, MNRAS, 433, 740
Singh K. P., Apparao K. M. V., Kraft R. P., 1994, ApJ, 421, 753
Thorstensen J. R., 1987, ApJ, 312, 739
White N. E., Marshall F., 1984, ApJ, 281, 354
White N. E., Mason K. O., 1985, Space Sci. Rev., 40, 157
Whitehurst R., King A. R., 1991, MNRAS, 249, 25
Wijnands R., Miller J. M., van der Klis M., 2002, MNRAS, 331, 60
Worthey G., 1994, ApJS, 95, 107
Yaqoob T., Ebisawa K., Mitsuda K., 1993, MNRAS, 264, 411

This paper has been typeset from a TEX/LATEX file prepared by the author.